JOURNAL OF VIROLOGY, Mar. 2005, p. 3391–3400 Vol. 79, No. 6
0022-538X/05/$08.00+0 doi:10.1128/JVI.79.6.3391–3400.2005

Single-Amino-Acid Substitutions in Open Reading Frame (ORF) 1b-nsp14 and ORF 2a Proteins of the Coronavirus Mouse Hepatitis Virus Are Attenuating in Mice

Steven M. Sperry,[1,2] Lubna Kazi,[3] Rachel L. Graham,[2,4] Ralph S. Baric,[5] Susan R. Weiss,[3] and Mark R. Denison[1,2,4]*

Departments of Pediatrics[1] and Microbiology and Immunology[4] and Elizabeth B. Lamb Center for Pediatric Research,[2] Vanderbilt University Medical Center, Nashville, Tennessee; Department of Microbiology, University of Pennsylvania School of Medicine, Philadelphia, Pennsylvania[3]; and Department of Epidemiology, School of Public Health, University of North Carolina, Chapel Hill, North Carolina[5]

Received 27 August 2004/Accepted 1 November 2004

A reverse genetic system was recently established for the coronavirus mouse hepatitis virus strain A59 (MHV-A59), in which cDNA fragments of the RNA genome are assembled in vitro into a full-length genome cDNA, followed by electroporation of in vitro-transcribed genome RNA into cells with recovery of viable virus. The "in vitro-assembled" wild-type MHV-A59 virus (icMHV-A59) demonstrated replication identical to laboratory strains of MHV-A59 in tissue culture; however, icMHV-A59 was avirulent following intracranial inoculation of C57BL/6 mice. Sequencing of the cloned genome cDNA fragments identified two single-nucleotide mutations in cloned genome fragment F, encoding a Tyr6398His substitution in open reading frame (ORF) 1b p59-nsp14 and a Leu94Pro substitution in the ORF 2a 30-kDa protein. The mutations were repaired individually and together in recombinant viruses, all of which demonstrated wild-type replication in tissue culture. Following intracranial inoculation of mice, the viruses encoding Tyr6398His/Leu94Pro substitutions and the Tyr6398His substitution alone demonstrated $\log_{10}$ 50% lethal dose (LD_{50}) values too great to be measured. The Leu94Pro mutant virus had reduced but measurable $\log_{10}$ LD_{50}, and the "corrected" Tyr6398/Leu94 virus had a $\log_{10}$ LD_{50} identical to wild-type MHV-A59. The experiments have defined residues in ORF 1b and ORF 2a that attenuate virus replication and virulence in mice but do not affect in vitro replication. The results suggest that these proteins serve roles in pathogenesis or virus survival in vivo distinct from functions in virus replication. The study also demonstrates the usefulness of the reverse genetic system to confirm the role of residues or proteins in coronavirus replication and pathogenesis.

Mouse hepatitis virus (MHV) is a widely studied model system for coronavirus replication and pathogenesis. Many strains of MHV have been isolated which differ in their tissue tropism and virulence. MHV strain A59 (MHV-A59) causes hepatitis in mice, but following intracranial inoculation is also capable of causing meningoencephalitis and chronic demyelinating disease (20). There have been many studies demonstrating the role of the structural proteins and nonstructural group-specific genes in replication and virulence, but only recently have genetic approaches been available to study viral determinants. Nevertheless, the complexity of coronavirus gene products makes it likely that new functions in replication and pathogenesis will be identified in the genome, including the replicase gene.

MHV possesses the largest positive-strand RNA genome of any known virus at ≈32 kb (Fig. 1). The 5′ two-thirds of the genome encodes the replicase in two overlapping open reading frames (ORFs), 1a and 1b, which, if translated in their entirety by a −1 ribosomal frameshifting mechanism, generate a ≈800-kDa polyprotein. The nascent replicase polyprotein is processed by virus-encoded proteinases to yield intermediate precursor and 16 mature cleavage products, including three proteinase activities, an RNA helicase/NTPase, and a putative RNA-dependent RNA polymerase.

Recent bioinformatics studies suggested homology of the 3′-most ORF 1b protein products, p59, p42, and p33 (nsp 14 to 16) to known cellular RNA processing enzymes. These include a 3′-5′ exonuclease of the DEDD superfamily for nsp14-p59, a poly(U)-specific endoribonuclease for nsp15-p42, and an *S*-adenosylmethionine-dependent ribose 2′-*O*-methyltransferase of the RrmJ family for p33 (43). These ORF 1b-encoded proteins have high primary amino acid sequence identity among all sequenced coronaviruses. Endonuclease activity has been demonstrated for recombinant purified poly(U)-specific endoribonuclease (16).

During MHV-A59 infection, six subgenomic mRNAs are transcribed from the 3′ 9.5 kb of the genome. These subgenomic mRNAs encode the structural proteins of MHV, including the spike glycoprotein (S), membrane protein (M), small membrane protein (E), and the nucleocapsid protein (N). Several other small open reading frames encode additional nonstructural proteins of largely unconfirmed function. These ORFs are referred to as "group-specific" ORFs because they are generally conserved in viruses in the same group in their sequence and expression but differ across groups. The MHV mRNA2 is translated to yield the ORF 2a protein, a 30-kDa nonstructural protein that was recently predicted,

* Corresponding author. Mailing address: Department of Pediatrics, Vanderbilt University Medical Center, D6217 MCN, Nashville, TN 37232-2581. Phone: (615) 343-9881. Fax: (615) 343-9723. E-mail: mark.denison@vanderbilt.edu.

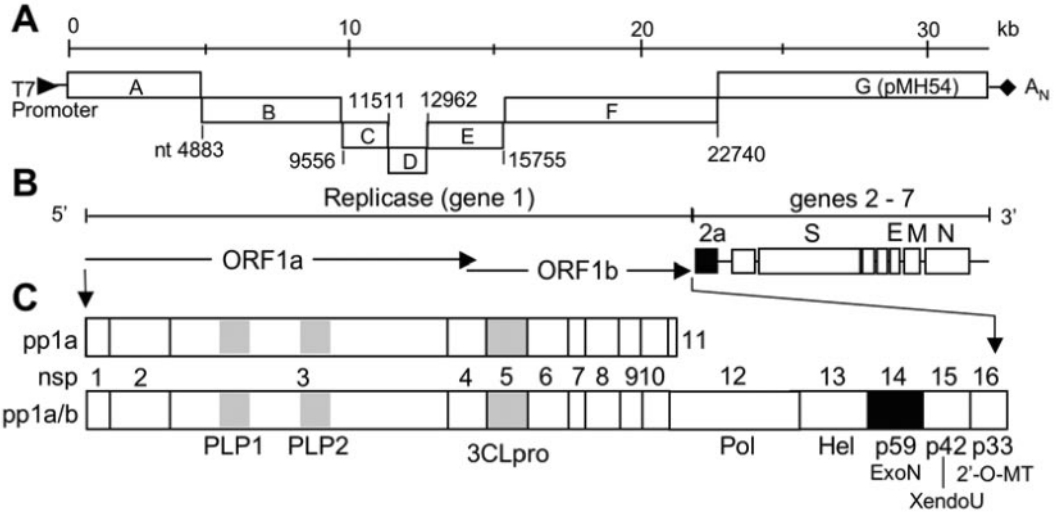

FIG. 1. MHV genome organization, proteins, and genome cDNA fragments. (A) The MHV reverse genetics system divides the genome into seven cDNA fragments with a T7 promoter at the beginning of fragment A and poly(A) tail at the end of the fragment G (pMH54). The junction of the fragments is indicated by nucleotide number. (B) The genome consists of seven genes. The replicase gene comprises the first 22 kb. Genes 2 to 7 are translated from subgenomic mRNA species (not shown). The relative locations of coding regions for the structural proteins S, E, M, and N are shown, as is the coding region for the group-specific ORF 2a 30-kDa protein. (C) The ORF 1a and frameshifted ORF 1a/b fusion polyproteins are depicted (pp1a and pp1ab, respectively). The protein domains of the replicase polyprotein are indicated by nonstructural protein number (nsp1 to 16) and by confirmed or predicted functions: PLP1 and 2, papain-like proteinases; 3CLpro, 3C-like proteinase; Pol, putative RNA-dependent RNA polymerase; Hel, helicase; ExoN, putative exonuclease; XendoU, putative poly(U)-specific endoribonuclease; 2′-O-MT, methyltransferase. Proteins with substitutions are shown as black rectangles.

based on conservation of specific residues, to be a cyclic phosphodiesterase, an RNA processing enzyme involved in tRNA maturation pathways (43).

Until recently, reverse genetics studies of MHV were performed exclusively with targeted recombination (18). This system remains a powerful and flexible system; however, it does not allow targeted mutagenesis of the 5′ 20 kb of the MHV genome, which comprises the replicase gene, since the recombination donor is an RNA molecule containing the 3′ ≈10 kb of the genome. A new reverse genetics system for MHV-A59 was recently described by Yount et al. that allows targeting of mutations to any portion of the genome but specifically to the replicase and the 5′ noncoding region of the genome (50). This reverse genetics approach divides the genome into seven cDNA fragments (A to G), which are ligated in vitro and transcribed in vitro into full-length infectious RNA genome, which is then electroporated into cells with recovery of recombinant virus. The recombinant wild-type infectious clone MHV-A59 (icMHV-A59) obtained from this approach is identical to laboratory strains of MHV-A59 in replication, protein processing, and genomic and subgenomic RNA synthesis in tissue culture (50). The cloned fragments have been mutated to introduce substitutions and deletions in the replicase polyprotein, with defined changes in protein processing and virus replication (11).

In the current study we initially sought to confirm the virulence of wild-type icMHV-A59 in mice, since it demonstrated wild-type replication in culture. Surprisingly, pilot studies with intracranial inoculation of C57BL/6 mice showed that wild-type icMHV-A59 caused only mild illness and no deaths, even at inoculation doses 100 times greater than that causing mortality with wild-type MHV-A59. Sequencing of the genome cDNA fragments A through G identified two single-nucleotide mutations resulting in amino acid substitutions, one in the replicase ORF 1b p59-nsp14 protein (Tyr6398His) and the other in the ORF 2a 30-kDa protein (Leu94Pro). Repair of the residues to the conserved consensus sequence restored virulence in mice to that of wild-type A59. Viruses retaining either or both substitutions were independently attenuated for virulence in mice while demonstrating replication in culture identical to wild-type MHV-A59. The attenuated mutants had decreased virus titers in mouse brains, with evidence in some mice of partial or complete reversion of the residues to the consensus wild-type sequence. The experiments have identified residues in the replicase and in the ORF 2a protein at which substitutions do not impact replication in culture but may be critical for virus survival and virulence in vivo. Further, the studies have resulted in a stably cloned consensus MHV genome with a completely characterized sequence that directs synthesis of virus with both wild-type replication in culture and virulence in animals.

MATERIALS AND METHODS

Viruses and cells. Delayed brain tumor (DBT) cells and baby hamster kidney cells expressing the MHV receptor (BHK-MHVR) were grown in Dulbecco's modified Eagle's medium containing 10% fetal calf serum. The BHK-MHVR cells were grown under G418 selection (0.8 mg/ml), as previously described (11, 50). For comparisons of animal virulence, engineered viruses as described below were compared with RA59, a recombinant wild-type MHV-A59 selected by targeted recombination (32, 33). This RA59 virus therefore contains the same 3′ 10 kb as all viruses in this study, since they were similarly derived from the pMH54 cloned sequence. In addition, RA59 has been shown to recapitulate the virulence of laboratory strains of "wild-type" MHV-A59 (33).

Reverse genetic engineering and recovery of recombinant MHV-A59. The reverse genetics system for MHV-A59 was used to generate engineered viruses and to modify the genome, as previously described (11, 50). Plasmids containing

TABLE 1. Primers for mutagenesis of bases 19400 and 22051

Primer	Sequence[a]	Purpose
19400 BsmBI Left	5′-CGTCTCG$_{19397}$TTG**T**ATGTTAACAAACATGCATTCCACACC$_{119426}$	Mutagenesis primer nt 19400
19400 BsmBI Right	5′-CGTCTCG$_{19400}$**A**CAAACTGCCACCATTACAGCCAGG$_{19376}$	Mutagenesis primer nt 19400
19400 Outer Left	5′-$_{18638}$GTGGTTCGAATTAGAATAGTACAAATGTTGTCAGACCACC$_{18677}$	Sense primer BsmBI Right
19400 Outer Right	5′-$_{19944}$TTTCTAAAGAGCTTAAGCTCGGGGTGGGGCCGAATA$_{19909}$	Antisense primer BsmBI Left
22051 BbsI Left	5GAAGACGC$_{22048}$TTC**T**TGATGTTAGAGGATTTGAAGAGTTGCA$_{22078}$	Mutagenesis primer nt 22051
22051 BbsI Right	5ǪǪGGAAGACGC$_{22051}$**A**GAACAAGGCATCTGCCAAGCATGTG$_{22026}$	Mutagenesis primer nt 22051
22051 Outer Left	5Ǫ$_{19921}$CCCCGAGCTTAAGCTCTTTAGAAATTTGAATATTGACGTG$_{19960}$	Sense primer BsmBI Right
22051 Outer Right	5ǪGTCGGATCCACTAGTAACGGCCGCCAGTGTGCTGGAATT	Antisense primer BsmBI Left pSMART vector sequence

[a] Underlined nucleotides indicate restriction enzyme recognition sites. Nucleotides in bold-point mutations introduced into the VUSS0 sequence to restore MHV-A59 consensus sequence. Subscript numbers indicate boundaries of genomic sequence.

cDNA fragments A through G of the MHV RNA genome were digested, and the gel-purified genome fragments were ligated in vitro to yield a full-length genome cDNA. The T7 transcription promoter at the 5′ end of fragment A was used to drive transcription of full-length genome RNA, including a templated poly(A) tail, with the mMessage mMachine T7 transcription kit (Ambion). A 50-μl reaction was assembled according to the manufacturer's instructions, but for our experiments was modified by supplementation with 7.5 μl of 30 mM GTP, and the transcription reaction was performed at 40.5°C for 25 min, 37.5°C for 50 min, and 40.5°C for 25 min.

The full-length MHV genome transcripts were then combined with in vitro transcripts of the viral nucleocapsid gene and 600 μl of BHK-MHVR cells in phosphate-buffered saline (10^7 cells/ml) in a 4-mm-gap cuvette, and three electrical pulses of 850 V at 25 μF were delivered to the mixture in a Bio-Rad Gene Pulser Xcell electroporator. Electroporated cells were seeded over a layer of 10^6 uninfected DBT cells in a 75-cm^2 flask and incubated at 37°C for 30 h. Virus viability was determined by the appearance of cell death, plaques, and confluent syncytium formation and by the recovery of infectious virus from medium supernatant that was detectable by plaque assay and by infection of cell monolayers. Recovered virus was maintained as population stocks following passage of the medium from electroporated cells and also by selection of plaques followed by amplification of plaqued clones as P1 stocks. The outcome is recovery of engineered recombinant viruses with wild-type or mutant sequence. Since no single term is adequately descriptive of the whole process, we will for this report refer to the viruses as recombinant viruses and by reference to mutations, with the understanding that all viruses were generated by the same process. The nomenclature infectious clone will be retained for the original wild-type cloned MHV (icMHV-A59) that is the basis for the studies in this report.

Sequencing MHV cDNA fragments. The infectious clone MHV cDNA fragments (A to G) were sequenced with a set of primers designed from the MHV genome (NCBI accession 1NC001846). Sequencing primers were created every 600 bp, beginning with the 5′ end, from both the sense and antisense strands. These primers generated overlapping sequences spanning the cDNA clones at least twice and up to four times in targeted regions. The plasmid vectors and cloned fragments A to G have been characterized previously, and further modifications to fragment F are reported below. The M13 forward and reverse primers were used to sequence the insert-vector junction of fragments A, F, and G, and primers SL1 and SR1 for the pSMART vector (Lucigen) were used for fragments B to E.

Sequencing was performed with an ABI Prism automated sequencer. The sequences were aligned and compared with MHV sequences from the NCBI database: NC001846 (MHV-A59 mutant C12 genome); X73559 (24), X51939 (5), M23256 (25), M18379 (26), S58172 (47), M16602 (7), and X00509 (44) (wild-type MHV-A59 sequences); M55148 (21) (MHV-JHM ORF 1a/b sequence); M57954 (37), M57953 (37), M28348 (41), and M34035 (37) (MHV-JHM ORF 2a sequences); AF201929 (MHV-2 genome) (36); and AF207902 (8), AF208066 (unpublished), and AF208067 (8) (MHV recombinant genomes).

Site-directed mutagenesis and repair of genome cDNA fragment F. Site-directed mutations were made in fragment F (nucleotides 15755 through nucleotides 22740 from the 5′ end of the MHV-A59 genome). Fragment F was digested from the pCR-XL-Topo vectors originally employed and blunt ligated into a restriction digested (KpnI and SacI) and filled in (T4 DNA polymerase) pSMART-LC-Amp (Lucigen) vector in which the multiple cloning site from pBluescript II KS+ (nucleotides 657 to 755) was inserted at the PCR cloning site between nucleotides 2025 and 1 in the linear vector. Mutational repair of ic-MHV-A59 genome nucleotide 19400 (C to T), nucleotide 22051 (C to T), or both was accomplished by PCR with the primers shown in Table 1 and methods as previously described (50). A 5′ BstBI and 3′ AflII site or a 5′ AflII and 3′ SpeI site were used to clone the PCR product with the C19400T repair or C22051T repair, respectively, into fragment F in the pSMART-LC vector. All mutations were sequence confirmed and demonstrated stable growth and maintenance of changes in *Escherichia coli* in this vector.

Reverse transcription-PCR and sequencing of viral RNA. For all sequencing of genome RNA, discrete viral plaques under agar were selected during plaque assays. Virus was aspirated from plaques, dispersed in 1 ml of gel saline, and used to infect DBT cells in 25-cm^2 flasks (≈3×10^6 cells) for 30 min, followed by addition of Dulbecco's modified Eagle's medium with 10% fetal bovine serum. When≈80% of the monolayer was involved in syncytia (12 to 24 h postinfection), the cells were lysed with Trizol reagent (Invitrogen) and total RNA was isolated according to the manufacturer's protocol.

An antisense primer complementary to nucleotides 22126 through 22144 of the MHV genome was used to generate viral cDNA from the total RNA with reverse transcription. The reverse transcription product was amplified by PCR with the same antisense primer and a sense primer complementary to nucleotides 19321 through 19338. This PCR product was then sequenced over nucleotide 19400 and nucleotide 22051 to confirm the sequences of all viruses recovered following electroporation and replication in culture or from the brains of infected mice.

Virus replication in DBT cells. For analysis of replication, DBT cells in two replicate 75-cm^2 flasks (≈10^7 cells) were infected at a multiplicity of infection of 5 PFU/cell or 0.01 PFU/cell with passage 1 (P1) stocks of plaque isolates. Virus was adsorbed for 30 min at room temperature with rocking, and cells were then washed three times with phosphate-buffered saline (10 min per wash). Medium was added, and the cells were incubated at 37°C. Samples of medium were collected at 1, 4, 8, 12, 16, 25, 30, 36, and 42 h postinfection, and viral titers were determined by plaque assay on DBT cells as described previously (17). For each virus and time point, results presented are the mean of two independent replicates and two measurements at each time point.

Inoculation of mice, virulence assays, and measurement of brain virus titers. All animal experiments used 4-week-old MHV-free C57BL/6 mice (Jackson Laboratory, Bar Harbor, Maine). Mice were anesthetized with isofluorane. For intracranial inoculation, the amount of virus designated in each experiment was diluted in phosphate-buffered saline containing 0.75% bovine serum albumin, and a total volume of 20 μl was injected into the left cerebral hemisphere. Mock-infected controls were inoculated similarly but with an uninfected cell supernatant at a comparable dilution.

Fifty percent lethal dose (LD_{50}) assays were performed as previously described (15). Mice were inoculated intracranially with three serial dilutions (10^3, 10^4, and 10^5 PFU) of plaque-purified RA59, wild-type icMHV-A59, or mutant virus VUSS0, VUSS1, VUSS2, or VUSS3. In two independent experiments, a total of 5 to 15 animals per dilution per virus were analyzed. Mice were examined for signs of disease or death on a daily basis for up to 21 days postinfection. LD_{50} values were calculated by the Reed-Muench method, as previously described (28). For the measurement of virus replication in mouse brains and livers, 10 mice for each virus were infected with 5×10^3 PFU intracranially. Five mice for each virus were sacrificed at day 5 and day 7 postinfection and perfused with 10 ml of phosphate-buffered saline, and the brains and livers were removed. Each organ was placed directly into 2 ml of isotonic saline with 0.167% gelatin (gel saline), weighed, and stored frozen at −80°C until virus titers were determined. Organs were homogenized, and virus titers were determined by plaque assay on DBT cell monolayers as previously described (15).

Viruses from brains were isolated from individual plaques, and their genomes were sequenced in the regions encompassing the residues of interest with reverse transcription-PCR as described in the previous section. Plaque isolates from brains of two different mice per virus were sequenced across 600 nucleotides, including the coding region for ORF 1a/b residue 6398 and ORF 2a residue 94 to confirm the sequences and identify any reversions or new mutations in flanking sequences. For viruses where one or more plaque-cloned isolate demonstrated changes from the input virus inoculum, virus plaque isolates from up to five additional mice were sequenced.

Nucleotide sequence accession number. The GenBank accession number for the VUSS3 virus described in this report is AY910861.

RESULTS

icMHV demonstrates wild-type replication in culture but is attenuated in vivo. It has been shown that the original recombinant wild-type icMHV-A59 recovered following electroporation of cells with genome RNA transcribed in vitro from assembled full-length genome cDNA has wild-type replication in cultured cells (11, 50). To determine the virulence of icMHV in mice, 10^5 PFU of icMHV or RA59 was used to infect mice by intracranial inoculation. RA59 is a recombinant virus obtained by targeted recombination and serves as a control wild-type virus (33). We chose this virus for comparison with recombinant wild-type icMHV-A59 since the pMH54 donor plasmid was used for targeted recombination and was also the sequence used to generate fragment G used in the in vitro assembly of full-length genome cDNA (18, 50). Thus, both RA59 and icMHV possess the identical 3′ 10 kb of sequence.

Viruses derived from targeted recombination with pMH54, specifically RA59, have been shown to possess wild-type growth and virulence following intracranial inoculation of mice (33). However, in the pilot experiment, while some mice had transient illness, no mice inoculated with recombinant wild-type icMHV-A59, even at doses 100 times the LD_{50} of wild-type A59, died. This surprising result suggested that new or unrecognized changes in icMHV arising during its recovery or passage in cells had resulted in loss of replication, virulence, or both in animals. Alternatively, we considered the possibility that new mutations introduced during propagation of the fragment A through G plasmids in *E. coli* had resulted in changes affecting virulence in animals. This lack of virulence was particularly surprising since multiple wild-type and mutant viruses engineered on this background have demonstrated growth, plaque, protein, and RNA phenotypes indistinguishable from laboratory strains of MHV-A59. Thus, we hypothesized that any changes in the virus genome would alter virulence in mice but not affect replication in culture.

Identification of attenuating mutations in recombinant wild-type icMHV-A59. To identify candidate mutations in wild-type icMHV-A59 that might have contributed to this loss of virulence, cloned genome cDNA fragments A through G cDNAs were sequenced bidirectionally with overlapping sets of primers, resulting in sequence covering the genome at least twice and in some cases up to four times. The sequences were then compared with the sequences of the original amplicons and with published sequences (50).

Examination of key marker mutations in the sequence shows that the lineage of the infectious clone genome is most similar to MHV-A59 virus isolates derived from virus first described by Sturman (23), in contrast to the MHV-A59 viruses from which the majority of the published wild-type sequence fragments were derived (2, 5–7, 25, 47). The cDNA fragment A to G sequences were compared with the genome sequence of the C12 mutant virus (23) (NCBI accession 1NC001846), which also was derived from the Sturman lineage (15). Previous sequencing of the C12 mutant virus identified five coding mutations, one silent mutation, and one mutation in an untranslated region compared to the wild-type MHV-A59 sequences that were distinct from variations in known virulent viruses (23). The infectious clone fragment cDNA sequences did not contain any of the seven mutations previously identified for the C12 mutant virus.

We did identify 26 differences that either resulted in no amino acid substitutions (silent) or were located in untranslated regions of the genome. Three coding mutations were identified in fragments A to G (Fig. 2A). Ten of the 26 silent or untranslated mutations were previously reported as engineered mutations in the cDNA fragments A to G to remove restriction sites or create unique junctions (49). An additional ten silent and one coding mutation were identified in fragment G, which was derived from the pMH54 plasmid (19, 50). The sequence of fragment G matched pMH54 with the exception of one silent mutation (A23441G) in the nonexpressed ORF 2b (HE) gene (sequence kindly provided by Paul Masters).

Since several studies have shown that viruses generated by targeted recombination with pMH54 or a derivative are virulent (9, 19, 33), we focused on the two novel mutations found in the first 22.7 kb of the genome. When all previously described mutations and consensus sequences were considered, the cDNA sequences identified two single-nucleotide coding mutations, both in fragment F, T19400C and T22051C. These two mutations have not been described in any submitted or published MHV-A59 sequences or in related MHV-2, MHV-JHM, or recombinant virus sequences (2, 4, 8, 9, 22, 23, 25, 38, 42). Furthermore, the wild-type MHV-A59 viruses from the Denison laboratory at Vanderbilt University and the Weiss laboratory at the University of Pennsylvania were sequenced by reverse transcription-PCR over these regions and found to have T19400 and T22051 (not shown).

The first of these mutations predicted a Tyr6398His amino acid substitution in the ORF 1ab polyprotein. The Tyr6398His substitution is found in the sequence encoding MHV ORF 1b p59-nsp14. The Tyr6398 residue is absolutely conserved for coronaviruses with determined sequence (not shown). The second mutation was a Leu94Pro amino acid substitution in the ORF 2a 30-kDa protein. While only group 2 coronaviruses encode the group-specific ORF 2a protein, within that group the viruses that possess an intact ORF 2a protein have conserved the Leu94 residue (not shown). Thus, sequencing of the genome fragment cDNAs identified two novel coding mutations at conserved residues that were candidates for attenuation of the wild-type icMHV-A59 virus.

Correction of candidate attenuating mutations in wild-type icMHV-A59. While it was formally possible that introduced or identified changes at noncoding (silent) or nontranslated nucleotides could account for the loss of virulence, we hypothesized that coding changes were more likely to affect replication or virulence. We restored the genome nucleotide sequences individually and in combination to the consensus wild-type sequences, C19400T and C22051T, both within fragment F, with site-directed PCR mutagenesis. Following sequence confirmation of the changes, the corrected sequences encoded

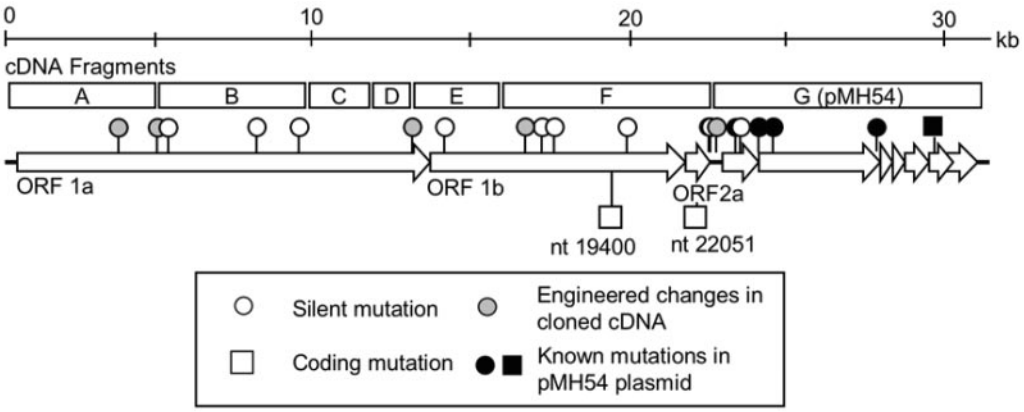

FIG. 2. Mutations identified by sequencing of the genome cDNA fragments. Genome fragments A through G are shown. The sequence was compared with published sequences as indicated in the text. The comparison identified 29 silent or nontranslated nucleotide differences (indicated by circles; a single circle can indicate multiple clustered differences) at nucleotides G3518A, G3521C, T4874A, C4877G, T4970C, T7982C, T9305C, A12962C, T12965A, C14014A, G17137A, G17140C, A17482G, T17524C, T19885C, A22608G, G22633T, T22739G, T22742C, C23393T, A23441G, T23964C, T23965C, G24447A, C24448T, T24450A, T27915C, C27918G, and T27920A. Three coding nucleotide differences were identified (indicated by squares) at nucleotides T19400C, T22051C, and T29650C. Ten of the silent mutations were engineered in the cloned fragments to introduce unique junctions or remove restriction sites (grey circles). The fragment G cDNA was derived from the pMH54 vector (19), and comparison of the sequences showed that of the eleven mutations identified, all had been previously noted (black circles and squares), except for a single silent mutation at nucleotide 23441 in the untranslated hemagglutinin-esterase (HE) pseudogene. Two novel coding differences in the cDNA fragments of the icMHV-A59 were identified at nucleotides 19400 and 22051 (white squares).

proteins with the wild-type residues Tyr6398 in ORF 1b p59-nsp14 and Leu94 in the ORF 2a 30-kDa protein. The corrected fragment F clones were used with fragments A, B, C, D, E, and G to assemble full-length genome cDNA in vitro, transcribe infectious genome RNA in vitro, electroporate cells, and recover virus (Fig. 3B).

The genome encoding both the uncorrected His6398 and Pro94 residues was designated VUSS0 to distinguish it from the reported recombinant wild-type icMHV-A59 and because of the probability that the changes were acquired after sequencing of the original fragments. VUSS1 encoded the corrected Tyr6398 (ORF 1b p59-nsp14) and mutant Pro94 (ORF 2a 30-kDa protein). VUSS2 encoded the mutant His6398 (ORF 1b p59-nsp14) and repaired Leu94 (ORF 2a 30-kDa protein). VUSS3 restored both consensus wild-type Tyr6398 and Leu94 residues. Recovered viruses were passaged three times in culture, and the sequence of genome RNA of purified virions was determined for both the population virus and plaque-cloned isolates. The sequences of the cloned mutant and repaired cDNA fragments were retained in the recovered viruses in all cases with no evidence of heterogeneity or other changes in the ≈3 kb incorporating both of the targeted nucleotides (data not shown).

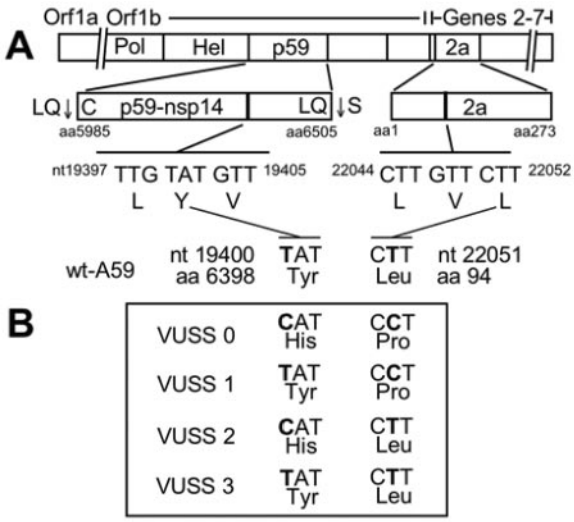

FIG. 3. Correction of substitution mutations in fragment F. (A) Mutations were corrected at nucleotides 19400 and 22051, changing the codons for amino acid 6398 in pp1a/b (amino acid 414 in p59-nsp14) and amino acid 94 in ORF 2a 30-kDa protein. (B) Mutant viruses were engineered with either a Tyr or His at amino acid residue 6398 in the ORF 1b p59-nsp14 paired with either a Leu or Pro at amino acid 94 in the ORF 2a 30-kDa protein. Four viruses were derived, representing the four possible combinations of amino acids at the two sites.

Uncorrected and corrected viruses exhibit wild-type replication in DBT cells. Single-cycle growth experiments were performed to compare the replication of putative wild-type and mutant viruses. When cells were infected at a multiplicity of infection of 5 PFU/cell, VUSS0, VUSS1, VUSS2, and VUSS3 all demonstrated peak titers, replication kinetics, cytopathic effect, and plaque morphology identical to wild-type A59 and the original recombinant wild-type icMHV-A59 (Fig. 4).

To test the possibility that mutant viruses had subtle replication differences detectable only during multiple-cycle growth, the growth assay was repeated with a multiplicity of infection of 0.01 PFU/cell. In direct comparison of two replicate infections for all viruses, the time to increase in virus titer and achievement of peak titer was delayed by 4 to 8 h compared with the high-multiplicity infection, confirming the multiple-cycle infection. However, as with the high-multiplicity infection, the replication kinetics and peak titers were overlap-

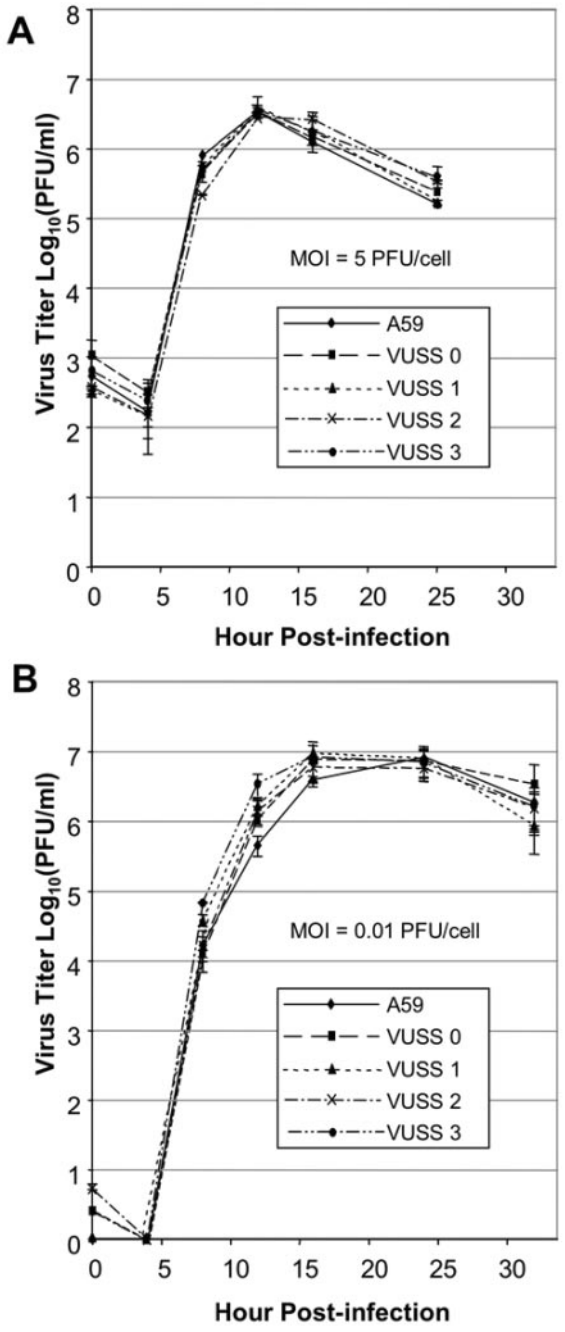

FIG. 4. Growth analysis of mutant viruses. Flasks of DBT cells (10^7 cells) were infected in duplicate with wild-type A59 (♦), VUSS0 (■), VUSS1 (▲), VUSS2 (X), and VUSS3 (●). (A) Multiplicity of infection of 5 PFU/cell. (B) Multiplicity of infection of 0.01 PFU/cell. Medium supernatant samples were obtained at 0, 4, 8, 12, 16, 24, and 32 h postinfection The plotted points represent the average of the viral titer determined by plaque assay for duplicate samples at each time point from two replicate infections.

ping. While it is still possible that there are extremely subtle alterations in replication, they are not detectable by our virological assays and suggest that in fact, replication in culture is wild type in viruses with substitutions at ORF 1b p59-nsp14 Tyr6398 and ORF 2a 30-kDa protein Leu94.

TABLE 2. Virulence in mice for wild-type RA59, corrected VUSS3, and mutants VUSS0, VUSS1, and VUSS2

Virus	Amino acid (p59/ORF2a)	Log_{10} LD_{50} (PFU)	
		Trial 1	Trial 2
RA59	Tyr/Leu	3.80	
VUSS0	His/Pro	>5.30	>5.30
VUSS1	Tyr/Pro	4.67	4.80
VUSS2	His/Leu	>5.30	>5.30
VUSS3	Tyr/Leu	3.80	3.80

Amino acid substitutions in the ORF 1b p59-nsp14 or ORF 2a 30-kDa protein attenuate virulence in vivo. Having demonstrated the stability and wild-type growth of VUSS0 (His6398/Pro94), VUSS1 (Tyr6398/Pro94), VUSS2 (His6398/Leu94), and VUSS3 (Tyr6398/Leu94), the virulence of the viruses was determined by intracranial inoculation of C57BL/6 mice in direct comparison with a virulent wild-type recombinant MHV-A59 (RA59). Virulence assays were carried out as described in Materials and Methods, and $\log_{10}$ LD_{50} values were calculated for each virus (Table 2). RA59 was virulent following intracranial inoculation, causing clinical disease and mortality in mice, with an LD_{50} of 3.8 $\log_{10}$, consistent with previous published virulence measurements with this virus (27, 33). In contrast, VUSS0 (His6398/Pro94) caused no death in inoculated mice and thus had an LD_{50} of >5.3 $\log_{10}$. The VUSS2 virus (His6398/Leu94) was also avirulent (LD_{50} > 5.3 $\log_{10n}$), indicating that the single Tyr6398His substitution was sufficient to eliminate virulence and raising the question of whether the substitution at Leu94 had any role in loss of virulence. When VUSS1 (Tyr6398/Pro94) was analyzed, it had an LD_{50} of 4.8 $\log_{10}$, demonstrating that it had an independent effect on virulence. To determine if repair of Tyr6398 and Leu94 restored virulence, VUSS3 (Tyr6398/Leu94) was analyzed and demonstrated virulence equivalent to RA59 (LD_{50} 3.8 $\log_{10}$), indicating that repair of Tyr6398 and Leu94 was necessary and sufficient to restore virulence following intracranial inoculation of mice.

Attenuated MHV viruses have reduced titers in mouse brains and livers at day 5 following intracranial inoculation. To determine if the mutant viruses were replicating in vivo, 10 mice per virus were inoculated intracranially with 5×10^3 PFU of VUSS0, VUSS2, VUSS3, and RA59. Mice were sacrificed on days 5 and 7 postinfection (five each on days 5 and 7 per virus), the brains were collected and homogenized, and virus was titered from clarified brain homogenates. In previous studies of virulent A59 strains following intracranial inoculation, peak replication occurs during the first week postinfection, peaking at day 5. Virus is usually not measurable by day 7, as was the case for all viruses in this study, with no measured virus titers by day 7 (not shown). At day 5 postinfection, RA59 and VUSS3 viruses had similar titers of 2.1×10^4 and 3.1×10^4 PFU per g of brain tissue, respectively (Fig. 5). In contrast, the attenuated VUSS0 and VUSS2 viruses had much less measurable virus at 5 days postinfection, with mean titers of 2.8×10^2 and 1.6×10^2 PFU/g of brain tissue, respectively. Virus from brains of mice infected with VUSS0 and VUSS2 could only be measured in nondiluted, clarified homogenates, but the results

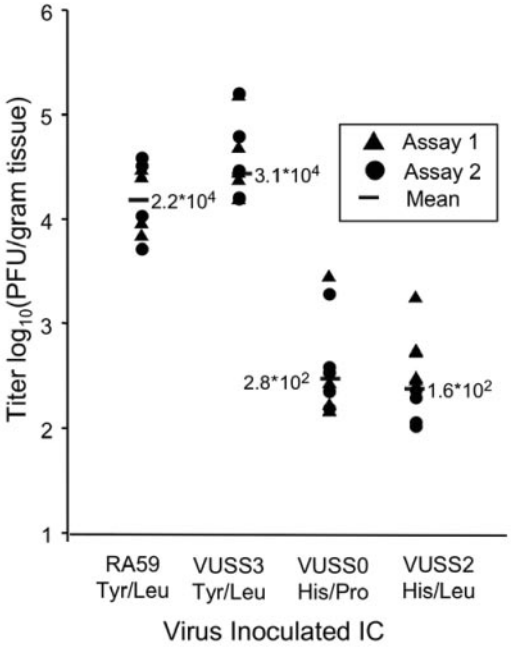

FIG. 5. Virus titers in brain tissue of infected mice, sacrificed at 5 days postinfection. Viral titers of clarified brain homogenates (five mice/virus) were determined by plaque assay in DBT cells. The titer for each sample was determined in two separate plaque assays, with each point the average of two measurements and normalized for brain mass. Means for five mice are indicated. Titers for VUSS0 and VUSS2 were reproducible in separate plaque assays, with plaques detected only in undiluted specimens.

were reproducible in replicate assays for both viruses. Thus, the loss of virulence of VUSS0 and VUSS2 was associated with decreased virus in the brains of infected mice at 5 days postinfection

MHV-A59 infection by an intracranial route also results in replication in the liver and hepatitis (27). To determine whether virus replication in the liver was detectable for mutant viruses, the livers from the same mice used to obtain brain titers at day 5 were homogenized and analyzed by plaque assay on DBT cells. For VUSS3, virus was detectable in four of five mice, with mean titers of 1.74×10^3 PFU per g of liver for the four mice with detectable virus. In contrast, for VUSS0 and VUSS2, no virus plaques were observed in either diluted or undiluted clarified homogenates. Whether replication was not occurring, was at such a low level as to be below limits of detection, or was rapidly cleared from the liver, the result indicates a replication defect for VUSS0 and VUSS2 in the liver as well as in the brain.

Retention and reversion of attenuating mutations in vivo. Since the amount of virus detected in the brains of mice infected with VUSS0 and VUSS2 was reduced, and since the mouse brain virus titers suggested significant variation in replication of specific viruses in different mice, we next determined if there was evidence of pressure for selection of reversion to wild-type sequences Tyr6398 and Leu94. From the plaque assay used to generate the data in Fig. 5, plaques were selected and inoculated into 25-cm^2 flasks of DBT cells. Total cellular RNA was harvested when the monolayers were greater than 80% involved with syncytia, and the RNA was reverse transcription-PCR sequenced across the ≈3 kb of the genome RNA coding sequence for both Tyr6398 and Leu94.

TABLE 3. Amino acid sequences of virus plaque isolates from mouse brains infected with RA59, VUSS3, VUSS0, and VUSS2[a]

Strain and mouse no.	Plaque isolate(s)	ORF1b p59-nsp14 aa6398	ORF2a 30-kDa aa94
RA59		**TYR**	**LEU**
Mouse 3	1	Tyr	Leu
Mouse 4	1	Tyr	Leu
VUSS3		**TYR**	**LEU**
Mouse 2	1	Tyr	Leu
Mouse 3	1	Tyr	Leu
VUSS0		**HIS**	**PRO**
Mouse 1	1, 3, 4	(Tyr)	(Leu)
Mouse 1	5	(Tyr)	Pro
Mouse 1	6	His	Pro
Mouse 2	1	His	Pro
Mouse 3	1, 2	His	Pro
Mouse 4	1, 2	His	Pro
Mouse 5	1, 2	His	Pro
VUSS2		**HIS**	**LEU**
Mouse 1	1, 2	His	Leu
Mouse 2	1, 2	His	Leu
Mouse 4	1, 3, 4, 5, 6	(Tyr)	(Pro)
Mouse 5	1	His	Leu

[a] Input sequence is indicated by bold capitals. Changes from input sequence are indicated by parentheses. VUSS0 mouse 5 isolates both contained an A to C mutation coding Asp to Ala change at aa 53 in ORF2a 30-kDa protein.

Initially, plaque isolates from each of two mice were sequenced for each input virus. The plaque isolates from mice infected with VUSS3 and RA59 maintained Tyr6398 and Leu94 in all cases, confirming the stability of the wild-type residues (Table 3). For both VUSS0 (His6398/Pro94) and VUSS2 (His6398/Leu94), plaque virus isolates from one mouse maintained the sequences of the infecting virus genomes. However, the plaque isolates from a second mouse for VUSS0 and VUSS2 showed changes at either or both residues.

We therefore sequenced multiple plaque isolates from the mice demonstrating changes as well as plaque isolates from up to five total mice for these viruses. For VUSS0, seven plaque isolates from a total of four mice retained the input His6398/Pro94 substitutions. However for mouse 4, one plaque isolate retained the substitutions, while three isolates showed reversion at both residues to wild-type Tyr6398/Leu94, and one plaque isolate showed partial reversion to Tyr6398/Pro94. For VUSS2, six plaque isolates from three mice retained the input residues His6398 and Leu94, while five isolates from one mouse showed changes at both residues, resulting in Tyr6398 and Pro94. This combination recapitulated that of engineered VUSS1, which was less virulent than wild-type or VUSS3 (Tyr6398/Leu94), but more virulent than the input VUSS2. While contamination cannot be entirely ruled out, VUSS1 was not included in this experiment, and all animals were inoculated with the same vial of VUSS2.

These results demonstrate that for the majority of infected mice, the input sequence and amino acids were retained, but reversion of either or both single-nucleotide coding mutations

in ORF 1b p59 and ORF 2a protein can occur during infection of mice, with evidence for selective pressure for more virulent wild-type or partial wild-type protein sequences. These results also support the conclusion that active replication of the attenuated mutants is occurring, since replication is required for generation and selection of changes, particularly of two independent mutations.

DISCUSSION

In this study we demonstrate that two single-nucleotide mutations that result in amino acid substitutions in the ORF 1b p59-nsp14 protein and the ORF 2a 30-kDa protein of MHV-A59 attenuate virulence in mice while having no measurable effect on virus replication in culture. By restoring the consensus wild-type sequences individually and in combination, we confirmed that the mutations are both independently and in combination attenuating in mice, although their phenotypes in DBT cell culture are indistinguishable from wild type MHV-A59. One of the mutations, encoding a Leu94Pro substitution in the ORF 2a 30-kDa protein, was only partially attenuating in the absence of any other changes. The second mutation, encoding a Tyr6398His substitution in the ORF 1b p59-nsp14 replicase protein, was completely attenuating independently or in combination with the first mutation. These results show that MHV genome RNA transcribed from an in vitro-assembled full-length cDNA can direct the synthesis of virus that has wild-type replication in culture and virulence in mice. The results further demonstrate the ability to use reverse genetic approaches to determine the contribution of specific proteins and residues to replication and virulence.

Identification of attenuating mutations and restoration of virulence of in vitro-assembled recombinant MHV. The discovery of two mutations in genome fragment F that attenuated virulence in mice but caused no detectable phenotype in cell culture was surprising. Since the sequence differed from that of the original fragment F at both nucleotides, we proposed that the mutations were selected for during propagation of the genome fragment F in the pTopo vector in *E. coli*. When we attempted to repair the fragment F cDNA to encode the consensus wild-type Tyr6398 and Leu94 residues by site-directed mutagenesis and propagation in *E. coli*, fragment F cDNA encoding His6398/Pro94 was recovered, supporting the conclusion that toxicity or other deleterious effects of the wild-type sequences in *E. coli* may have selected for the mutations.

We therefore subcloned fragment F into the pSMART-LCAmp vector (Lucigen), which subsequently allowed repair of the mutations and has remained stable during propagation in *E. coli*. The sequencing of the fragments also demonstrated that cloned genome fragments A, B, C, D, E, and G (pMH54) are stable during propagation in *E. coli*, with no evidence of deletion, truncation, or deleterious mutations. In addition, the wild-type replication and virulence of VUSS3 containing the corrected fragment F confirm that the strategy for assembly of cloned fragments, in vitro transcription of genome RNA, and electroporation of RNA into cells is clearly able to generate stably virulent virus. Thus, it will be possible to engineer changes in single fragments while maintaining a highly stable sequence in other fragments. It will also be possible, as we have previously demonstrated, to directly compare sequences from rescued viruses with the fragments specifically used for assembly and thereby identify reversions or compensating mutations introduced by the virus. The ability to reintroduce the original mutation and any candidate compensating mutations will allow rapid testing and confirmation of the changes and their relevance to replication and virulence. Finally, the results provide a basis for comparison with other viruses, both natural variants and viruses derived by any reverse genetic approaches, by providing the completely characterized sequence of a stably cloned MHV-A59 genome of a virus with wild-type replication in culture and virulence in vivo.

The observed outcome of intracranial infection in mice with the mutant or partially corrected viruses was greatly reduced virulence, as measured by the LD_{50}. This global decrease in virulence could have resulted from decreased replication, decreased virulence independent of replication, or altered immune response. Host cell proteins have been shown to interact with the genome during viral RNA synthesis (40, 51). MHV has been shown to utilize mitogen-activated protein kinase signaling in the cell and eIF4E phosphorylation to promote virus production (1). MHV also utilizes components of cellular autophagy during replication (34). Furthermore, it has been reported that MHV specifically suppresses the translation of some cellular mRNAs but not others (46). Thus, the ORF 1b p59-nsp14 and/or ORF 2a 30-kDa proteins might normally interact with or modulate the expression of host cellular factors required for viral replication in the mouse, leading to a reduction of viral replication.

Alternatively, the proteins might be involved in modulating the host immune response. Differences in encephalitis disease severity for different strains of MHV have been associated with the differential regulation of cytokines and the innate immune response stimulated by the viruses (31, 35). Hence, it is possible that in the presence of the mutant proteins, cytokines or other antiviral components are differentially activated, leading to an altered immune response.

The titer of infectious virus in the brains and livers at day 5 postinfection was reduced or undetectable in mice infected with VUSS0 and VUSS2 compared to the corrected VUSS3. However, the detection of infectious virus in brains at day 5, along with the reversion or partial reversion to the wild-type sequences observed for both VUSS0 and VUSS2, demonstrates that replication was occurring and that there was pressure for selection of more fit virus. Further, both VUSS0 and VUSS2 demonstrated wild-type growth in culture even at a low multiplicity of infection, indicating that the viral machinery necessary for entry, replication, assembly, and release is intact. Thus, if the observed decrease in virulence is due to replication defects, they would likely be due to cell-specific requirements that are not present in the murine DBT or hamster BHK cell lines. This in turn would suggest that the ORF 1b p59-nsp14 and ORF 2a 30-kDa proteins may function during interactions with specific cell types. Whether replication, pathogenesis, or both are directly affected, it is clear that the virus is specifically attenuated in vivo by changes in the proteins that appear to be dispensable for in vitro replication.

ORF 2a 30-kDa and ORF 1b p59-nsp14 proteins in replication and virulence. The ORF 2a 30-kDa protein is one of a group of group-specific proteins (2a, 4, and 5a) that have been reported to be nonessential for replication in culture (29, 37, 47, 48). The small ORF 7-encoded group I coronavirus-specific protein of the porcine coronavirus transmissible gastroenteritis virus is nonessential for replication but does influence in vivo replication and virulence (30). For MHV, no direct function in pathogenesis has been established for the group-specific proteins. A recombinant MHV lacking ORF s 2a, 4, and 5a has been shown to be avirulent in mice, but this virus is also defective for replication in vitro, making it difficult to interpret

the in vivo attenuation (10). Furthermore, a recombinant MHV-JHM lacking expression of ORF 4 appeared to display neurovirulence equal to wild-type JHM (29).

The MHV ORF 2a 30-kDa protein is only found among group 2 coronaviruses. The wild-type Leu94 is completely conserved among group 2 viruses that possess the ORF 2a protein. While this protein also has no known function, it has been reported to be a nonstructural protein that is cytosolic and non-membrane associated (3, 52). A similarity search produced an alignment of the protein to three consensus sequence elements for GTP and ATP nucleotide binding (25). The Leu94 amino acid residue aligns with a hydrophobic consensus sequence element. Another more recent bioinformatics analysis has predicted the protein to be a cyclic phosphodiesterase based on limited similarity to the catalytic motifs of two domains adjacent to the nucleotide binding elements (43). While none of these functions has been experimentally confirmed, our result showing partial attenuation of virulence with a single amino acid substitution and restoration of virulence following repair of the mutation strongly suggests a role for direct functions or virus cell interactions critical for virus survival and disease in the host.

Comparison of multiple coronaviruses indicates that the replicase gene may express both group-specific proteins (nsp1-p28 and nsp2-p65 of group 2 viruses), as well as moderately to highly conserved orthologs of MHV nsp3-16 in all coronaviruses. This organization and conservation of sequence have been the basis for concluding that the nsp3 through nsp16 proteins serve critical roles in the replication of coronaviruses, a conclusion confirmed for the papain-like proteinase activities of nsp3, the 3C-like proteinase activity of nsp4, and the helicase activities of nsp13 in addition to the highly likely but as yet unconfirmed polymerase activity of nsp12. More recently, RNA processing activities have been predicted for nsps 14, 15, and 16. nsp14-p59 has highly conserved orthologs in all coronaviruses that have been predicted to be an exoribonuclease of the DEDD superfamily (43). This prediction is based on primary amino acid sequence identity of three motifs containing, among other features, the putative catalytic aspartic and glutamic acid residues necessary for the exonuclease activity.

It is unknown what role the predicted p59-nsp14-exoribonuclease might have in the context of viral replication. The Tyr6398His substitution identified in this study was 140 amino acids downstream of the last predicted exoribonuclease catalytic motif. It is possible that an amino acid substitution distal to the putative active motifs could still alter or abolish the core protein function. If so, this would suggest that protein function of nsp14 is not required for MHV replication in culture. However, experiments in our laboratory with substitutions and deletions at other residues of p59-nsp14 suggest that the protein is likely required for replication (Sperry et al., unpublished results). Alternatively, ORF 1b p59-nsp14 may serve more than one role in replication and pathogenesis. The nsp14 orthologs of all sequenced coronaviruses have a high degree of overall identity and similarity, and more specifically, the Tyr6398 residue is 100% conserved in all coronaviruses sequenced to date. Experiments in progress will define if other substitutions at Tyr6398 and across the putative catalytic and zinc finger residues of nsp14 allow recovery of viable virus with wild-type replication or demonstrate various degrees of impairment or an absolute requirement for the intact protein.

Finally, the conservation of identified residues will make it possible to determine if similar substitutions are attenuating in other coronaviruses. The recent establishment of a reverse genetic system for severe acute respiratory syndrome coronavirus should make it possible to test whether substitutions at the conserved Tyr residues allow wild-type growth in culture and attenuation in animal models. If so, this could represent an approach for stable attenuation of severe acute respiratory syndrome coronavirus virulence by combining this powerfully attenuating mutation with other independently attenuating alleles across the genome

ACKNOWLEDGMENTS

We thank Ming Ming Chua, who performed initial testing of recombinant viruses in mice, Richard Watson for preparing the brain and liver lysates, and Sarah Brockway and Jennifer Sparks for critical reading of the manuscript.

This work was supported by NIH grants AI26603 (M.R.D.), AI17418 (S.R.W.), AI23946 (R.S.B.), and Training Grant in Cellular, Biochemical, and Molecular Sciences 5T32GM00855 (R.L.G.).

REFERENCES

1. **Banerjee, S., K. Narayanan, T. Mizutani, and S. Makino.** 2002. Murine coronavirus replication-induced p38 mitogen-activated protein kinase activation promotes interleukin-6 production and virus replication in cultured cells. J. Virol. **76:**5937–5948.
2. **Bonilla, P. J., A. E. Gorbalenya, and S. R. Weiss.** 1994. Mouse hepatitis virus strain A59 RNA polymerase gene ORF 1a: heterogeneity among MHV strains. Virology **198:**736–740.
3. **Bredenbeek, P. J., A. F. Noten, M. C. Horzinek, and W. J. Spaan.** 1990. Identification and stability of a 30-kDa nonstructural protein encoded by mRNA 2 of mouse hepatitis virus in infected cells. Virology **175:**303–306.
4. **Bredenbeek, P. J., C. J. Pachuk, A. F. Noten, J. Charite, W. Luytjes, S. R. Weiss, and W. J. Spaan.** 1990. The primary structure and expression of the second open reading frame of the polymerase gene of the coronavirus MHV-A59; a highly conserved polymerase is expressed by an efficient ribosomal frameshifting mechanism. Nucleic Acids Res. **18:**1825–1832.
5. **Bredenbeek, P. J., C. J. Pachuk, A. F. H. Noten, J. Charite, W. Luytjes, S. R. Weiss, and W. J. M. Spaan.** 1990. The primary structure and expression of the second open reading frame of the polymerse gene of the coronavirus MHV-A59; a highly conserved polymerase is expressed by an efficient ribosomal frameshifting mechanism. Nucleic Acids Res. **18:**1825–1832.
6. **Budzilowicz, C. J., and S. R. Weiss.** 1987. In vitro synthesis of two polypeptides from a nonstructural gene of coronavirus mouse hepatitis virus strain A59. Virology **157:**509–515.
7. **Budzilowicz, C. J., and S. R. Weiss.** 1987. In vitro synthesis of two polypeptides from a nonstructural gene of coronavirus mouse hepatitis virus, strain A59. Virology **157:**509–515.
8. **Das Sarma, J., L. Fu, S. T. Hingley, M. M. Lai, and E. Lavi.** 2001. Sequence analysis of the S gene of recombinant MHV-2/A59 coronaviruses reveals three candidate mutations associated with demyelination and hepatitis. J. Neurovirol. **7:**432–436.
9. **Das Sarma, J., L. Fu, J. C. Tsai, S. R. Weiss, and E. Lavi.** 2000. Demyelination determinants map to the spike glycoprotein gene of coronavirus mouse hepatitis virus. J. Virol. **74:**9206–9213.
10. **de Haan, C. A., P. S. Masters, X. Shen, S. Weiss, and P. J. Rottier.** 2002. The group-specific murine coronavirus genes are not essential, but their deletion, by reverse genetics, is attenuating in the natural host. Virology **296:**177–189.
11. **Denison, M. R., B. Yount, S. M. Brockway, R. L. Graham, A. C. Sims, X. Lu, and R. S. Baric.** 2004. Cleavage between replicase proteins p28 and p65 of mouse hepatitis virus is not required for virus replication. J. Virol. **78:**5957–5965.
12. **Easterfield, A. J., B. M. Austen, and O. M. Westwood.** 2001. Inhibition of antigen transport by expression of infected cell peptide 47 (ICP47) prevents cell surface expression of HLA in choriocarcinoma cell lines. J. Reprod. Immunol. **50:**19–40.
13. **Gombold, J. L., S. T. Hingley, and S. R. Weiss.** 1993. Identification of peplomer cleavage site mutations arising during persistence of MHV-A59. Adv. Exp. Med. Biol. **342:**157–163.
14. **Harris, R. S., K. N. Bishop, A. M. Sheehy, H. M. Craig, S. K. Petersen-Mahrt, I. N. Watt, M. S. Neuberger, and M. H. Malim.** 2003. DNA deamination mediates innate immunity to retroviral infection. Cell **113:**803–809.
15. **Hingley, S. T., J. L. Gombold, E. Lavi, and S. R. Weiss.** 1994. MHV-A59 fusion mutants are attenuated and display altered hepatotropism. Virology **200:**1–10.

16. **Ivanov, K. A., T. Hertzig, M. Rozanov, S. Bayer, V. Thiel, A. E. Gorbalenya, and J. Ziebuhr.** 2004. Major genetic marker of nidoviruses encodes a replicative endoribonuclease. Proc. Natl. Acad. Sci. USA **101:**12694–12699.
17. **Kim, J. C., R. A. Spence, P. F. Currier, X. T. Lu, and M. R. Denison.** 1995. Coronavirus protein processing and RNA synthesis is inhibited by the cysteine proteinase inhibitor e64dd. Virology **208:**1–8.
18. **Koetzner, C. A., M. M. Parker, C. S. Ricard, L. S. Sturman, and P. S. Masters.** 1992. Repair and mutagenesis of the genome of a deletion mutant of the coronavirus mouse hepatitis virus by targeted RNA recombination. J. Virol. **66:**1841–1848.
19. **Kuo, L., G. J. Godeke, M. J. Raamsman, P. S. Masters, and P. J. Rottier.** 2000. Retargeting of coronavirus by substitution of the spike glycoprotein ectodomain: crossing the host cell species barrier. J. Virol. **74:**1393–1406.
20. **Lavi, E., D. H. Gilden, Z. Wroblewska, L. B. Rorke, and S. R. Weiss.** 1984. Experimental demyelination produced by the A59 strain of mouse hepatitis virus. Neurology **34:**597–603.
21. **Lee, H.-J., C.-K. Shieh, A. E. Gorbalenya, E. V. Koonin, N. LaMonica, J. Tuler, A. Bagdzhadhzyan, and M. M. C. Lai.** 1991. The complete sequence (22 kilobases) of murine coronavirus gene 1 encoding the putative proteases and RNA polymerase. Virology **180:**567–582.
22. **Lee, H. J., C. K. Shieh, A. E. Gorbalenya, E. V. Koonin, N. La Monica, J. Tuler, A. Bagdzhadzhyan, and M. M. Lai.** 1991. The complete sequence (22 kilobases) of murine coronavirus gene 1 encoding the putative proteases and RNA polymerase. Virology **180:**567–582.
23. **Leparc-Goffart, I., S. T. Hingley, M. M. Chua, X. Jiang, E. Lavi, and S. R. Weiss.** 1997. Altered pathogenesis of a mutant of the murine coronavirus MHV-A59 is associated with a Q159L amino acid substitution in the spike protein. Virology **239:**1–10.
24. **Lu, Y. Q., and M. R. Denison.** 1997. Determinants of mouse hepatitis virus 3C-like proteinase activity. Virology **230:**335–342.
25. **Luytjes, W., P. J. Bredenbeek, A. F. Noten, M. C. Horzinek, and W. J. Spaan.** 1988. Sequence of mouse hepatitis virus A59 mRNA 2: indications for RNA recombination between coronaviruses and influenza C virus. Virology **166:** 415–422.
26. **Luytjes, W., L. S. Sturman, P. J. Bredenbeek, J. Charite, B. A. van der Zeijst, M. C. Horzinek, and W. J. Spaan.** 1987. Primary structure of the glycoprotein E2 of coronavirus MHV-A59 and identification of the trypsin cleavage site. Virology **161:**479–487.
27. **Navas, S., S. H. Seo, M. M. Chua, J. D. Sarma, E. Lavi, S. T. Hingley, and S. R. Weiss.** 2001. Murine coronavirus spike protein determines the ability of the virus to replicate in the liver and cause hepatitis. J. Virol. **75:**2452–2457.
28. **Navas, S., and S. R. Weiss.** 2003. Murine coronavirus-induced hepatitis: JHM genetic background eliminates A59 spike-determined hepatotropism. J. Virol. **77:**4972–4978.
29. **Ontiveros, E., L. Kuo, P. S. Masters, and S. Perlman.** 2001. Inactivation of expression of gene 4 of mouse hepatitis virus strain JHM does not affect virulence in the murine CNS. Virology **289:**230–238.
30. **Ortego, J., I. Sola, F. Almazan, J. E. Ceriani, C. Riquelme, M. Balasch, J. Plana, and L. Enjuanes.** 2003. Transmissible gastroenteritis coronavirus gene 7 is not essential but influences in vivo virus replication and virulence. Virology **308:**13–22.
31. **Parra, B., D. R. Hinton, M. T. Lin, D. J. Cua, and S. A. Stohlman.** 1997. Kinetics of cytokine mRNA expression in the central nervous system following lethal and nonlethal coronavirus-induced acute encephalomyelitis. Virology **233:**260–270.
32. **Phillips, J. J., M. Chua, S. H. Seo, and S. R. Weiss.** 2001. Multiple regions of the murine coronavirus spike glycoprotein influence neurovirulence. J. Neurovirol. **7:**421–431.
33. **Phillips, J. J., M. M. Chua, E. Lavi, and S. R. Weiss.** 1999. Pathogenesis of chimeric MHV4/MHV-A59 recombinant viruses: the murine coronavirus spike protein is a major determinant of neurovirulence. J. Virol. **73:**7752–7760.
34. **Prentice, E., W. G. Jerome, T. Yoshimori, N. Mizushima, and M. R. Denison.** 2003. Coronavirus replication complex formation utilizes components of cellular autophagy. J. Biol. Chem. **279:**10136–10141.
35. **Rempel, J. D., S. J. Murray, J. Meisner, and M. J. Buchmeier.** 2004. Differential regulation of innate and adaptive immune responses in viral encephalitis. Virology **318:**381–392.
36. **Sarma, J. D., L. Fu, S. T. Hingley, and E. Lavi.** 2001. Mouse hepatitis virus type-2 infection in mice: an experimental model system of acute meningitis and hepatitis. Exp. Mol. Pathol. **71:**1–12.
37. **Schwarz, B., E. Routledge, and S. G. Siddell.** 1990. Murine coronavirus nonstructural protein ns2 is not essential for virus replication in transformed cells. J. Virol. **64:**4784–4791.
38. **Schwarz, B., E. Routledge, and S. G. Siddell.** 1990. Murine coronavirus nonstructural protein ns2 is not essential for virus replication in transformed cells. J. Virol. **64:**4784–4791.
39. **Seo, S. H., E. Hoffmann, and R. G. Webster.** 2002. Lethal H5N1 influenza viruses escape host antiviral cytokine responses. Nat. Med. **8:**950–954.
40. **Shi, S. T., P. Huang, H. P. Li, and M. M. Lai.** 2000. Heterogeneous nuclear ribonucleoprotein A1 regulates RNA synthesis of a cytoplasmic virus. EMBO J. **19:**4701–4711.
41. **Shieh, C. K., H. J. Lee, K. Yokomori, M. N. La, S. Makino, and M. M. Lai.** 1989. Identification of a new transcriptional initiation site and the corresponding functional gene 2b in the murine coronavirus RNA genome. J. Virol. **63:**3729–3736.
42. **Shieh, C. K., H. J. Lee, K. Yokomori, N. La Monica, S. Makino, and M. M. Lai.** 1989. Identification of a new transcriptional initiation site and the corresponding functional gene 2b in the murine coronavirus RNA genome. J. Virol. **63:**3729–3736.
43. **Snijder, E. J., P. J. Bredenbeek, J. C. Dobbe, V. Thiel, J. Ziebuhr, L. L. Poon, Y. Guan, M. Rozanov, W. J. Spaan, and A. E. Gorbalenya.** 2003. Unique and conserved features of genome and proteome of SARS-coronavirus, an early split-off from the coronavirus group 2 lineage. J. Mol. Biol. **331:**991–1004.
44. **Spaan, W., H. Delius, M. Skinner, J. Armstrong, P. Rottier, S. Smeekens, B. A. van der Zeijst, and S. G. Siddell.** 1983. Coronavirus mRNA synthesis involves fusion of noncontiguous sequences. EMBO J. **2:**1839–1844.
45. **Spann, K. M., K. C. Tran, B. Chi, R. L. Rabin, and P. L. Collins.** 2004. Suppression of the induction of alpha, beta, and lambda interferons by the NS1 and NS2 proteins of human respiratory syncytial virus in human epithelial cells and macrophages. J. Virol. **78:**4363–4369.
46. **Tahara, S. M., T. A. Dietlin, C. C. Bergmann, G. W. Nelson, S. Kyuwa, R. P. Anthony, and S. A. Stohlman.** 1994. Coronavirus translational regulation: leader affects mRNA efficiency. Virology **202:**621–630.
47. **Weiss, S. R., P. W. Zoltick, and J. L. Leibowitz.** 1993. The ns 4 gene of mouse hepatitis virus (MHV), strain A 59 contains two ORF s and thus differs from ns 4 of the JHM and S strains. Arch. Virol. **129:**301–309.
48. **Yokomori, K., and M. M. C. Lai.** 1991. Mouse hepatitis virus S RNA sequence revels that nonstructural proteins ns4 and ns5a are not essential for murine coronavirus replication. J. Virol. **65:**5605–5608.
49. **Yount, B., K. M. Curtis, E. A. Fritz, L. E. Hensley, P. B. Jahrling, E. Prentice, M. R. Denison, T. W. Geisbert, and R. S. Baric.** 2003. Reverse genetics with a full-length infectious cDNA of severe acute respiratory syndrome coronavirus. Proc. Natl. Acad. Sci. USA **100:**12995–13000.
50. **Yount, B., M. R. Denison, S. R. Weiss, and R. S. Baric.** 2002. Systematic assembly of a full-length infectious cDNA of mouse hepatitis virus strain A59. J. Virol. **76:**11065–11078.
51. **Yu, W., and J. L. Leibowitz.** 1995. A conserved motif at the 3′ end of mouse hepatitis virus genomic RNA required for host protein binding and viral RNA replication. Virology **214:**128–138.
52. **Zoltick, P. W., J. L. Leibowitz, E. L. Oleszak, and S. R. Weiss.** 1990. Mouse hepatitis virus ORF 2a is expressed in the cytosol of infected mouse fibroblasts. Virology **174:**605–607.